

Optical properties of gelatin/TGS composites

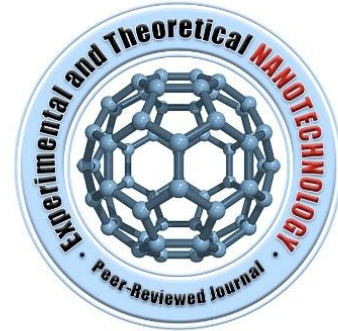
A. M. Shehap¹, Kh.H. Mahmoud¹, M.F.H. Abdelkader²,
Tarek M. El-Basheer^{3,*}

¹Department of Physics, Faculty of Science, Cairo
University, Giza, Egypt

²Department of Biophysics, Faculty of Science, Cairo
University, Giza, Egypt

³Department of Acoustics, Mass and Force Metrology Division, National institute for
standards (NIS), Giza, Egypt

*) Email: tarek31.uv@gmail.com



Received 19 March. 2017; Accepted 22 March 2017; Published 15 May 2017

Films of pure Gelatin and five Gelatin samples doped with the ferroelectric material triglycine sulphate (TGS) at various concentrations of 2, 4, 6, 8 and 10 wt. %TGS by weight have been prepared using the solvent-casting technique. Ultraviolet-visible (UV-vis) absorption spectra were measured in the range 190-900nm. The UV-Visible spectra show some shift in the absorption edge indicating change in optical band gap energy. The optical transitions were found mainly to be indirect allowed transitions and the optical band gaps (E_{opt}) were determined. Measuring the absorbance, transmittance and reflectance of Gelatin, TGS and their composites permitted the calculation of the refractive index (n). The refractive index dispersion curve of composite films obeys the single-effective oscillator model (Wemple-DiDomenico model).

Keywords: TGS; Absorption edge; Band tail.

1. INTRODUCTION

Recent studies have shown that Gelatin-based films with various additives have good potential for applications in a number of optoelectronic devices [1]. Gelatin containing ammonium dichromate is a well-known holographic recording material and is used in some holographic recording systems [2,3]. Gelatin-based films have been used in grating couplers [4], multiplexed gratings [5] and optical interconnections [6]. Poled Gelatin-nitro phenol compositions have shown good electro optical properties [7]. Pyroelectric and dielectric

properties of Synthetic polypeptide triglycerol-Gelatin films were investigated [8-10]. Gelatin is a relatively low-cost protein, industrially produced all over the world and that have excellent film forming properties. Mainly because of that, this protein is being extensively explored in edible and/or biodegradable films production and characterization studies, pure [11-15], or blended with other biopolymers [16, 17]. However, those Gelatin-based films present the typical characteristics of biopolymer-based films made with hygroscopic plasticizers are highly affected by room conditions, mainly relative humidity. Due to hygroscopic character of this material, relative humidity changes may lead to alteration of its moisture content affecting consequently the film properties, as water has a strong plasticizing effect on polymeric systems [18, 19]. Gelatin is nutritionally rich in glycine, proline, hydroxyproline, but lacking tryptophan and containing small amounts of other important amino acids, Fig. 1 shows the structure of Gelatin. It has a primary structure based on a repeating sequence (glycine/proline/hydroxyproline) [20]. Triglycine sulphate $[(\text{NH}_2\text{CH}_2\text{-COOH})_3 \text{H}_2\text{SO}_4]$ is one of the most extensively studied material as it possesses excellent pyroelectric and ferroelectric properties. It exhibits strong absorption in most of the infrared region. At room temperature, its pyroelectric coefficient value is very large [21]. This crystal is suitable to make speed broad band infrared pyroelectric detectors and vidicon. Also, it is a technologically important material for carbon dioxide laser (10.6 μm) and hydrogen cyanide laser (337 μm). Triglycine sulphate (TGS) finds wide applications as IR detectors, storage devices and laser devices [22-24], owing to its excellent ferroelectric properties. Triglycine sulphate (TGS) is an important material used in the fabrication of high sensitivity infrared detectors at room temperature [25-27]. Ferroelectricity in most of these compounds is related to the ordering of protons in their structure. The crystal structure of TGS was reported by Hoshino et al. [28] and the Curie temperature was reported a typical second-order ferroelectric phase transition at the Curie point $T_c=49^\circ\text{C}$ [29,30]. TGS family crystals belong to the monoclinic system with the polar point symmetry group P21 in the Ferroelectric phase, spontaneous polarization P_s arises along the b-axis and P2m in the Para electric phase [31,32]. The ferroelectric properties of the TGS Family crystals have been extensively studied with doping it with various amino acids [33, 34]. TGS crystal has some disadvantages over doped TGS crystal such as i) the ferroelectric domain possesses high mobility at room temperature therefore it is necessary to stabilize domains, ii) easy depolarization by electrical, mechanical and thermal means and iii) microbial contamination with time during the growth. In order to overcome these disadvantages

and to improve the ferroelectric properties of TGS, variety of dopants such as amino acids, Organic and inorganic compounds have been introduced in TGS crystal. Scientific and technical developments are closely linked with the implementation of new materials. One of the most important advances is the composite material or hetero phase material. The composites have steadily gained growing importance during the last decade [35]. One class of these polymer composites has high modulus, high strength and low cost that makes it useful instead of fiber-reinforced composites that are relatively expensive and are intended for demanding structural application. On the other hand, a special class of composites based on polymers and ferroelectrics has been proved to have extraordinary properties. Therefore, polymer/ferroelectric composites would a good replacement for either class alone and would have the desirable properties of both materials [35]. Accordingly, the composite of Gelatin and TGS is expected to be a good candidate for new material with enhanced physical properties. UV-visible (UV-vis) spectra and particularly the absorption edge, band tail and optical constants are used to provide a good idea about structural changes of the composite films(gelatin/TGS). In the present work, gelatin/TGS films with different additive (TGS) percentage have been prepared by casting technique. The objective is to study the effect of the dopant throughout all the samples towards the optical properties.

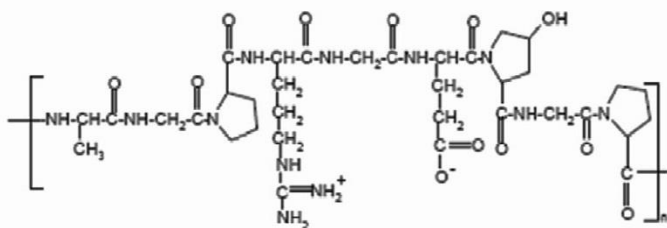


Figure 1 Structure of gelatin.

2. MATERIALS USED

The macromolecule used for film production was: Gelatin (Type B, and Bloom=190-200) was supplied by E.Merck(Darmstadt, Germany), and the average molecular-weight ≈ 100.000 gm/mol. From the specifications, Gelatin was composed of glycine (27%), proline and hydroxyproline (25%), glutamic acid (10%), arginine (8%), alanine (9%), aspartic acid (6%) and other amino acids (15%).

The ferroelectric material triglycine sulphate (TGS) was purchased from Acros Organic. Its molecular weight is 170. TGS crystals in the ferro- and paraelectric phase, 3-4 cm long.

2.1 Sample preparation

In order to obtain a film of pure Gelatin, Gelatin was dissolved in distilled water and in water bath at temperature of 37°C with continuous stirring for 30 min. until completely dissolved, then pour it into Petri dishes and cooled down at room temperature. Polymer/ ferroelectric composite samples were prepared by weighed amount of Gelatin and TGS in powder form with different concentrations 2, 4, 6, 8 and 10 wt. % TGS then dissolved them in distilled water at room temperature using magnetic stirrer. Thickness of films was measured using digital micrometer with sensitivity 0.01mm. Five to ten thickness measurements were taken on each film and took the average. Thus, thin films of appropriate thickness (≈ 0.05 mm) were cast on to Petri dishes and then dried at room temperature for about two or three days until the solvent completely evaporated. Films were cut into slab pieces and prepared to fit the cell of measuring techniques. All Films were conditioned in a desiccators with saturated solutions of NaBr(58% relative humidity) at 25°C until used.

2.2 Measuring techniques

The ultraviolet/visible absorption spectra of the samples under investigation were recorded on a Perkin Elmer 4B spectrophotometer over the range 190-1100 nm.

3. RESULTS AND DISCUSSION

3.1 Optical properties

Ultraviolet – visible spectra

The study of optical absorption spectra has proved to be very useful for elucidation and understanding the electronic structure of material through the determination of the optical band gaps. The data of transmittance can be analysed to determine optical constants such as

refractive index, extinction coefficient and dielectric constants which are of considerable importance for application in integrated optical devices such as switches and filters modulators, etc.... .Figure 2 shows the electronic absorption spectra (UV-visible spectra) of Gelatin, TGS and their composites (2, 4, 6, 8 and 10 wt. % TGS) at wavelength within the Uv-vis. range of 190 – 900nm. One can see that two essential maximum peaks at 230 and 275nm for the Gelatin absorption spectra. These two peaks may be attributed to the electronic transition $\pi \rightarrow \pi^*$ at 230nm, and the second due to $n \rightarrow \pi^*$ at 275nm. The strong absorption at 230nm that can be attributed to the non-aromatic amino acids while the observed band at the longest wavelength interval(≈ 275 nm) may be due to the presence of aromatic amino acids[37,38].

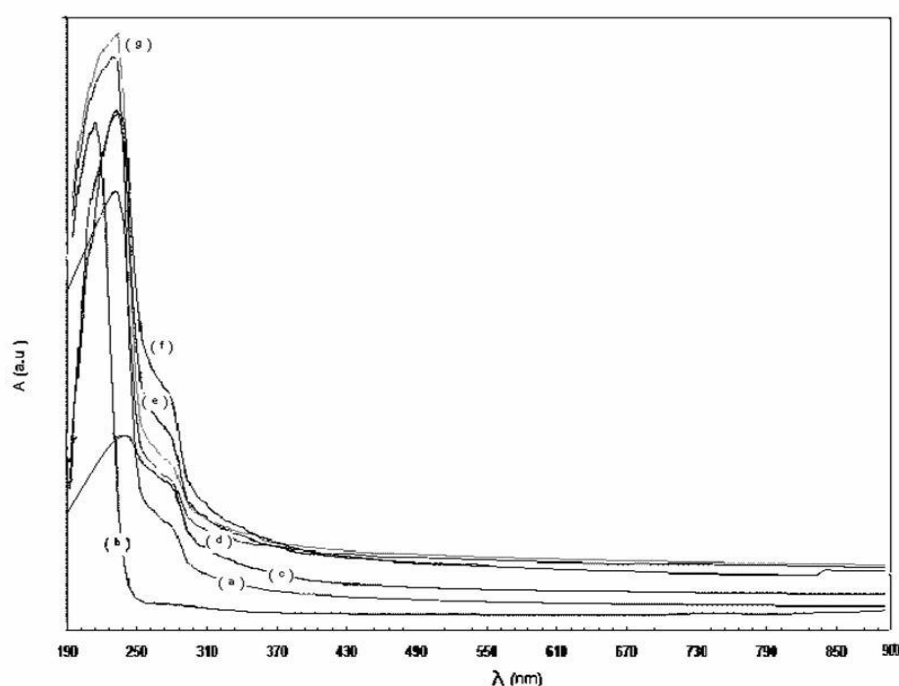


Figure.2 Absorption spectra for (a) pure gelatin (b) pure TGS (c) 2 (d) 4 (e) 6 (f) 8 and (g) 10 wt.% TGS.

The absorption spectra of TGS shows an essential maximum peak at 215nm that may be attributed to $\pi \rightarrow \pi^*$ transition which is characteristic of the crystalline state [39, 40]. The absorption spectra of the composite samples give two maximum transition peaks; one is sharp

while the other is shoulder-like band. There is small shifting in their wavelength assignment that depending upon the TGS concentration. It is clear that the sample (2wt%TGS) has the lower absorbance than the two pure samples and the other composites. Various optical transitions between these energy levels and the conduction or valence bands are found, together with transition between these impurity levels. Electron states can also be delocalized by increasing the impurity concentration and this is because the large spatial extension of the impurity states- the overlap of impurity wave function and thus delocalization occurs at low impurity concentration. For small impurity concentrations, transitions from the valence band to the impurity levels, or from these levels to the continuum of states, are possible leading to sharp absorption lines, together with transition between states. The type and degree of absorption depend on the type of impurity present and its concentration [41]. On the other hand there is little absorbance is detected through the visible spectral range for all the investigated samples (i.e the all samples are transparency in the visible region).

Optical Parameters:

The absorption coefficient $\alpha(\lambda)$ is calculated from the experimental optical absorption spectra using the relation [42]

$$\alpha(\lambda) = \frac{1}{d} \ln \frac{1}{T} \quad (1)$$

where d is the film thickness and T is the transmittance. The absorption coefficient was obtained with an error $\pm 4\%$. The values of $\alpha(\lambda)$ for TGS sample are in good agreement with that previously reported[43-45].

The fundamental absorption edge is an important feature of absorption spectra of crystalline and amorphous materials. The absorption process involves the transition of electrons from valence band to conduction band [47]. At the point where there is an abrupt rise in absorption called fundamental absorption edge.

Figure 3 shows the dependence of the absorption coefficient on the photon energy for pure Gelatin and TGS as well as their composite samples.

The absorption edge in many disordered materials follows the Urbach rule [47] given by

$$\alpha(\nu) = \beta \exp(h\nu / \Delta E) \tag{2}$$

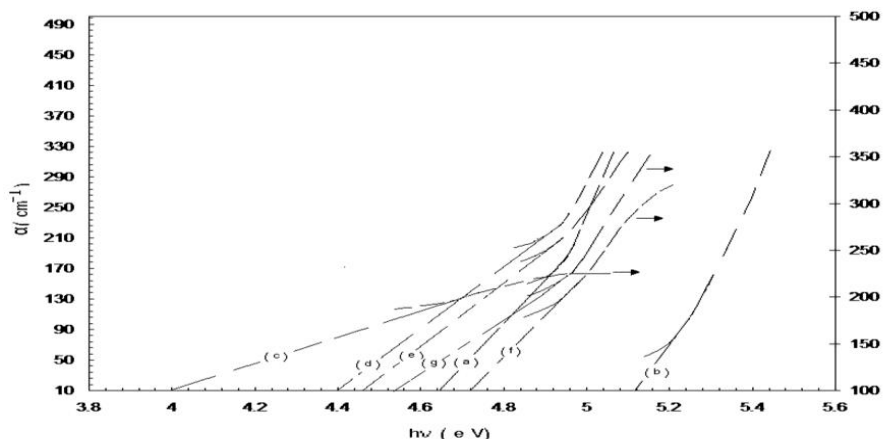


Figure.3 The absorption coefficient α as a function of photon energy $h\nu$ for (a) pure gelatin (b) pure TGS (c) 2 (d) 4 (e) 6 (f) 8 and (g) 10 wt.% TGS.

From Fig. 3, it is clear that $\alpha(h\nu)$ exhibits a steep rise near the absorption edge and then rapidly increases in a straight line relationship in the relatively high α -region. This rapid increase of α is attributed to inter band transitions. The intercept of extrapolation to zero absorption with photon energy axis was taken as the value of the absorption edge. These values are listed in Table 1. The values of the absorption edge for composite samples are less than the two pure samples. The reduction of absorption edge of the composite samples compared to pure Gelatin can be attributed to the changes of the crystallinity induced by TGS, which is consistent with earlier X-ray diffraction data. In addition, this may reflect the induced changes in the number of available final states according to composite composition.

The origin of the exponential dependence of absorption coefficient on photon energy ($h\nu$) has been suggested by Tauc[48]that it arises from electron transitions between localized states where the density of localized states is exponentially dependent on energy.

Table1 Values of absorption edges of Gelatin, TGS and their composite samples.

| | Sample | Absorption edge(eV) | |
|----------|---------------|----------------------------|-----------------|
| For the | Gelatin | 4.64 | samples |
| the | TGS | 5.12 | investigated in |
| the | 2wt.% TGS | 4.00 | present work, |
| | 4wt.% TGS | 4.40 | exponential |
| | 6wt.% TGS | 4.48 | behaviour is |
| | 8wt.% TGS | 4.72 | observed |
| [47]. | 10wt.% TGS | 4.56 | obeying |
| tails in | | | Urbach relation |
| semi- | | | The absorption |
| | | | amorphous and |
| | | | crystalline |

materials can be interpreted in terms of the Dow-Redfield effect [48] or the Urbach's[46] relation. The band tailing behavior may be caused by many kinds of structure disorder such as point defect, alloying disorder, inhomogeneous strain, exciton absorption and impurity levels in the middle of band gap [50].

Figure 4 shows the relation between $\ln\alpha$ and $h\nu$ for Gelatin, TGS and their composite samples. The straight lines obtained suggest that the absorption follows the quadratic relation for inter-band transitions [51] and the Urbach rule is obeyed. The values of band tail ΔE were calculated

from the slopes of these lines and are listed in Table 2. The values of band tails ΔE for the composites are higher than both of pure materials (Gelatin and TGS) and it is worth to pay an attention for the composite sample 2wt.% TGS that has the largest value of the band tail among the other composites. It has been assumed that the amorphous state is a perturbed crystalline-state (i.e a modified band picture could be considered for non-crystalline system [52]. The formations of composite samples probably induce tails in the density of states by perturbing the band edge via a deformation potential, coulomb interaction and by forming localized band states [51].

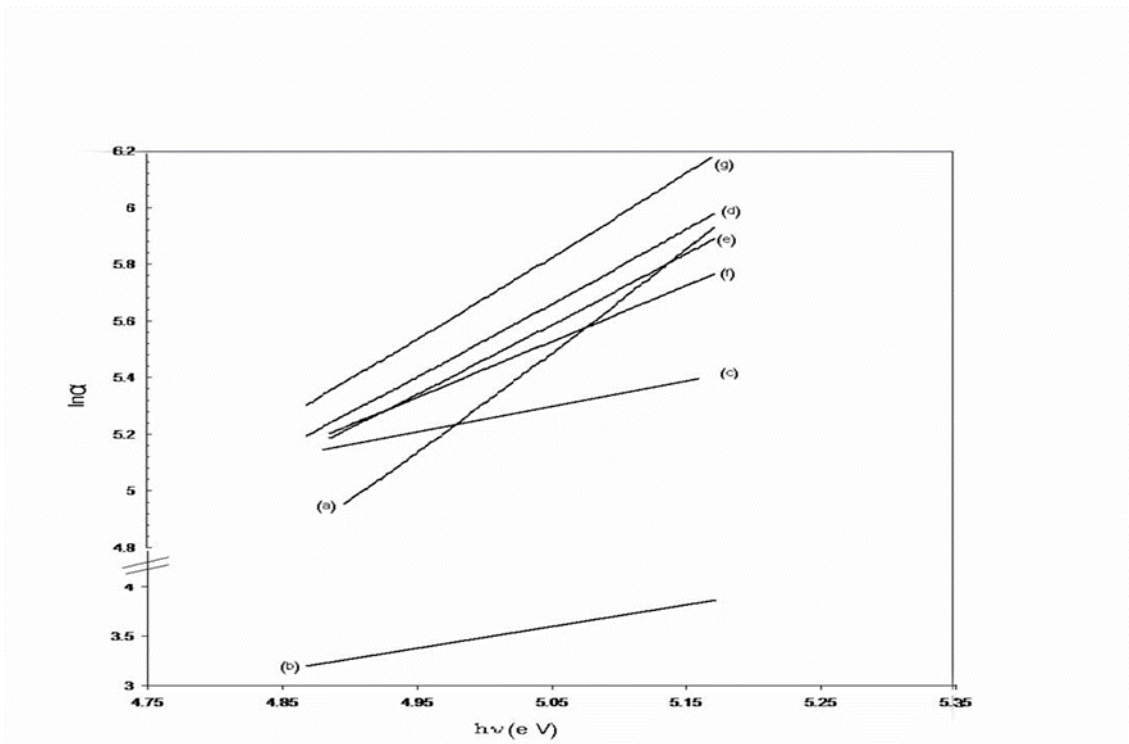


Figure 4 Relation between $\ln(\alpha)$ and $(h\nu)$ for (a) pure gelatin (b) pure TGS (c) 2 (d) 4 (e) 6 (f) 8 and (g) 10 wt.% TGS.

| Table 2 | Sample | Band tail(e V) | Values of band tails of TGS and their composite |
|-------------------|---------------|-----------------------|---|
| Gelatin, samples. | Gelatin | 0.40 | |
| | TGS | 0.35 | |
| | 2wt.% TGS | 0.95 | |
| | 4wt.% TGS | 0.55 | |
| | 6wt.% TGS | 0.53 | |
| | 8wt.% TGS | 0.65 | |
| | 10wt.% TGS | 0.51 | |

Thus, the model [52] based on electronic transition between localized states in the band edge tails and the density state of which is assumed to fall exponentially with energy, is preferable. In the high energy side, for the inter band transitions near the fundamental edge, the absorption coefficient α is given by the following relationship [47]

$$\alpha = \frac{B}{h\nu} (h\nu - E_g)^n \quad (3)$$

where $h\nu$ is the photon energy, E_g is the optical energy gap and (n) is an exponent characterizing the optical absorption process. For direct allowed transition $n=1/2$, for direct forbidden transition $n=3/2$, for indirect allowed transition $n=2$, for indirect forbidden transitions $n=3$.

The simplest way to deduce the type of transition is to examine the value of n which relates $(h\nu)$ to $(\alpha h\nu)$ with a straight line relationship. The values of $n=2$ showed the linear most fit of equation(3).

So, the optical absorption data for Gelatin, TGS and their composite samples show an indirect allowed transition.

The absorption coefficient for indirect allowed transition α_i can be expressed as

$$\alpha_i = \alpha_a + \alpha_e \tag{4}$$

α_a and α_e Being respectively, the contribution due to absorption and emission of phonons and they take the forms.

$$\alpha_a = \frac{B(T)(h\nu - E_{gi} + E_p)^2}{h\nu} \tag{5}$$

$$\alpha_e = \frac{B'(T)(h\nu - E_{gi} - E_p)^2}{h\nu} \tag{6}$$

where E_{gi} is the indirect energy gap, E_p the phonon energy, $B(T)$ and $B'(T)$ are constants nearly independent of photon energy and known as disorder parameters.

The spectral distribution of $(\alpha h\nu)^{1/2}$ for Gelatin, TGS and their composites are shown in Fig. 5. It is clear from the figure that the total absorption exhibits a long varying tail at low energies. Values of the optical energy gap for pure and composite samples obtained by extrapolating the linear regions to $(\alpha h\nu)^{1/2} = 0$. These values are listed in Table 3.

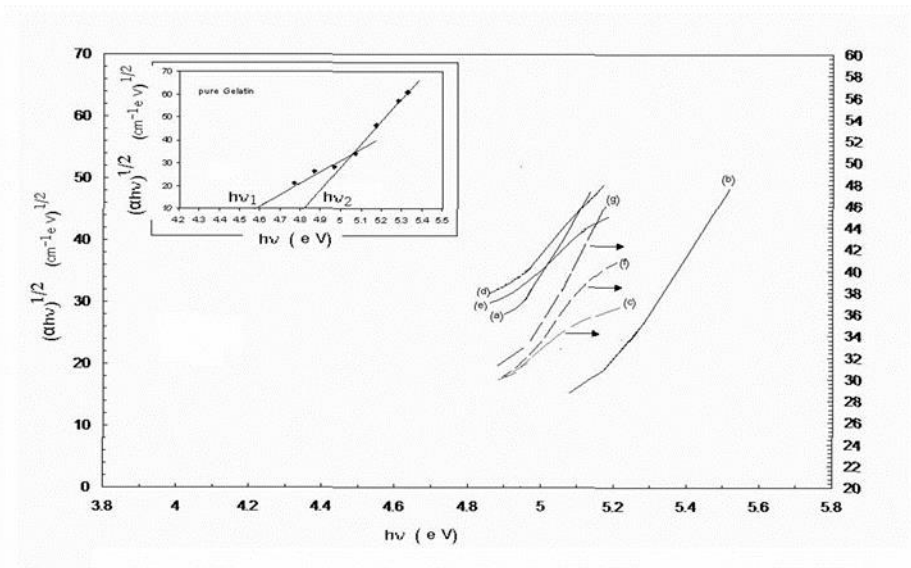


Figure 5 The plots of variations $(\alpha h\nu)^{1/2}$ against photon energy ($h\nu$) for (a) pure gelatin (b) pure TGS (c) 2 (d) 4 (e) 6 (f) 8 and (g) 10 wt.% TGS.

Table 3 Values of optical energy gaps and phonon energies of Gelatin, TGS and their composite samples.

| Sample | Optical energy gap(e V) | Phonon energy (e V) |
|------------|-------------------------|---------------------|
| Gelatin | 4.70 | 0.20 |
| TGS | 5.00 | 0.28 |
| 2wt.% TGS | 4.10 | 0.14 |
| 4wt.% TGS | 4.45 | 0.18 |
| 6wt.% TGS | 4.35 | 0.16 |
| 8wt.% TGS | 4.19 | 0.15 |
| 10wt.% TGS | 4.59 | 0.17 |

The graph (Fig.5) representing the relation between $(\alpha h\nu)^{1/2}$ and $h\nu$ may be resolved into two straight lines. The straight line obtained at lower photon energy corresponding to phonon absorption processes and cut photon energy axis at $h\nu_1 = (E_{gi} - E_p)$. The other line corresponding to the phonon emission and cut the x-axis at $h\nu_2 = (E_{gi} + E_p)$.

The study of the optical constant in the vicinity of the absorption edge has yielded significant information on the role of various atoms or molecules in the composite system. It is known that, if a multiple reflections are neglected, the reflectance R of the samples can be calculated from the experimental measured values of the transmittance T and absorbance using the following equation[54],

$$R = [1 - (T \exp A)]^{1/2} \quad (7)$$

Also, the extinction coefficient (k) is given as

$$k = \left(\frac{\alpha \lambda}{4\pi} \right) \tag{8}$$

Using the values of k and R , the refractive index can be determined from the following equation[54]

$$n = [(1 + R)/(1 - R)] \pm \{ [(R + 1)/(R - 1)]^2 - (1 + k^2) \}^{1/2} \tag{9}$$

Reasonable values form may be evaluated by considering the plus sign of the last equation.

Figure 6 shows the $n(\lambda)$ spectra from 350 to 850nm for all investigated samples. It is clear from the figure that the refractive index decreases slightly with increasing wavelength, and the changes become larger at shorter wavelengths showing the typical shape of a dispersion curve. The values of n is reached at longer wavelength to constant value n_0 . The values of n_0 for different investigated sample are given in Table 4. The values of refractive index n_0 for the composite samples are higher than both gelatin and TGS.

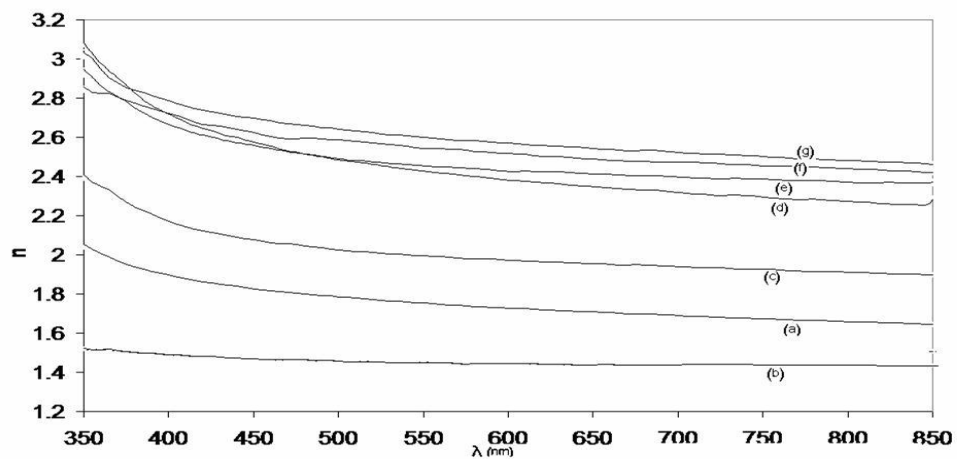


Fig 6 Variation in refractive index (n) with wavelength (λ nm) for (a) pure gelatin (b) pure TGS (c) 2 (d) 4 (e) 6 (f) 8 and (g) 10 wt.%TGS.

Table 4 Values of refractive index of Gelatin, TGS and their composite samples.

| Sample | Refractive index n_0 |
|---------------|--|
| Gelatin | 1.64 |
| TGS | 1.50 |
| 2wt.% TGS | 1.89 |
| 4wt.% TGS | 2.40 |
| 6wt.% TGS | 2.43 |

| | |
|------------|------|
| 8wt.% TGS | 2.45 |
| 10wt.% TGS | 2.52 |

The refractive index is one of the fundamental properties of a material and is closely related to the electronic polarizability of ions and the local field inside the material. Perhaps the polarization direction of doping molecules of TGS associated with gelatin molecules in the composite samples plays a much more important role in improving the bond polarizabilities [55]. It is worth to mention that the production of high refractive index, transparent composite film is essential for development of many photonic applications such as Ultra-low-loss optical waveguides and more efficient gain or non-linear optical devices.

Figure 7 shows the extinction coefficient k as a function of wavelength for both pure materials and their composite samples. The dependence preserves that behavior of the absorption coefficient for all samples near the absorption edges.

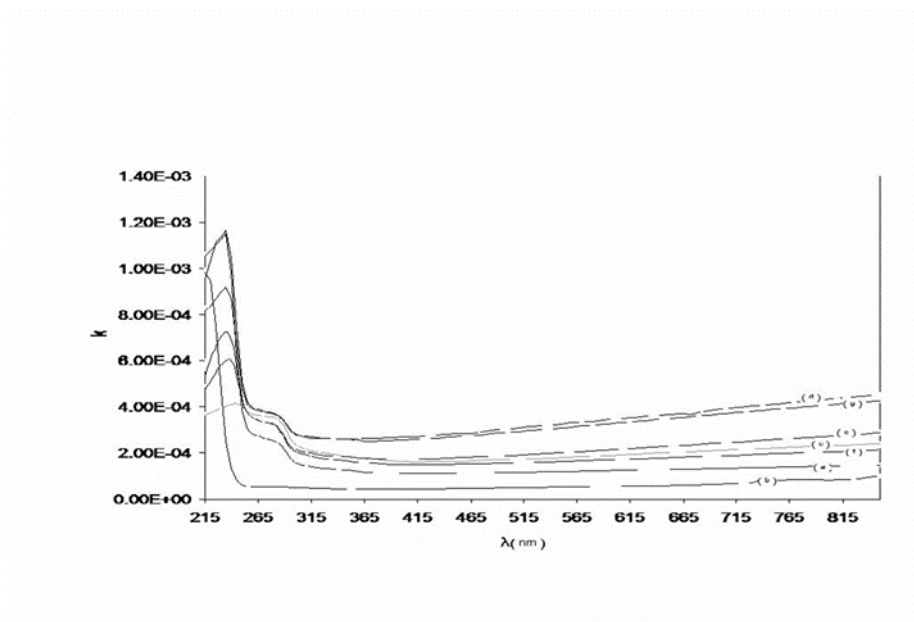


Figure 7 Variation in extinction coefficient (k) with wave length(λ) for (a) pure gelatin (b) pure TGS (c) 2 (d) 4 (e) 6 (f) 8 and (g) 10 wt.%TGS.

Parameters of the single-effective-oscillator model:

The imaginary dielectric constant ϵ_i is the optical constant accessible to physical interpretation using result of refractive index dispersion below the inter-band absorption edge corresponding to the fundamental electronic excitation spectrum.

Wemple and Domenico[56] have analysed more than 100 widely different solids and liquids using single-effective-oscillator fit of the form

$$\epsilon_r(E) = 1 + \frac{F}{(E_0^2 - E^2)} \tag{10}$$

Where the single oscillator energy (E_0) having a straight forward relation with dipole strength(F) and the corresponding transition frequencies of all oscillators. By a special combination of parameters Wemple and Domenico[56] have defined a parameter E_d such that it is a measure of the strength of intra-band optical transitions:

$$E_d = \frac{F}{E_0} \tag{11}$$

In the transparent region, equation (10) together with equations (11)

$$\epsilon_r = n^2 - k^2 \text{ and } \epsilon_i = 2nk \tag{12}$$

Neglecting values of k in the transparent region we can have

| Sample | E_0 , (eV) | E_d , (eV) | F | λ_0 , (nm) | n_∞ | S_0 , (nm ⁻²) | ϵ'_∞ |
|-----------|--------------|--------------|--------|--------------------|------------|--------------------------------|--------------------|
| Gelatin | 6.91 | 23.06 | 135.1 | 213.36 | 1.7 | 4.15*10 ⁻⁵ | 2.89 |
| TGS | 6.9 | 7.25 | 49.68 | 179.34 | 1.54 | 4.06*10 ⁻⁵ | 2.37 |
| 2wt.%TGS | 6.15 | 43.93 | 269.99 | 203.87 | 1.9 | 6.27*10 ⁻⁵ | 3.61 |
| 4wt.%TGS | 5.58 | 45.41 | 253.38 | 221.77 | 2 | 6.09*10 ⁻⁵ | 4 |
| 6wt.%TGS | 5.45 | 47.015 | 256.4 | 227.06 | 2.35 | 8.70*10 ⁻⁵ | 5.52 |
| 8wt.%TGS | 5.19 | 48.52 | 251.81 | 238.43 | 2.4 | 8.37*10 ⁻⁵ | 5.76 |
| 10wt.%TGS | 5.04 | 57.16 | 294.08 | 247.5 | 2.55 | 8.98*10 ⁻⁵ | 6.5 |

$$\epsilon_r(E) = n^2(E) = 1 + \frac{E_d E_0}{E_0^2 - E^2} \tag{13}$$

$$(n^2 - 1) = \frac{E_d E_0}{E_0^2 - E^2} \tag{14}$$

$$(n^2 - 1)^{-1} = \frac{E_0^2}{E_d E_0} - \frac{E^2}{E_d E_0} = \left(-\frac{1}{E_d E_0}\right)E^2 + \frac{E_0}{E_d} \tag{15}$$

By plotting $(n^2-1)^{-1}$ versus E_2 (eV). The result would be a straight line with negative slope $(1/E_d E_0)$ and intersection (E_0/E_d) . The data was fitted to the best straight line as shown in Fig. 8. The estimated values of E_0 and E_d for pure materials Gelatin and TGS and their composite samples are given in Table5.

Table 5 Single-Oscillator parameters of Gelatin, TGS and their composite sample

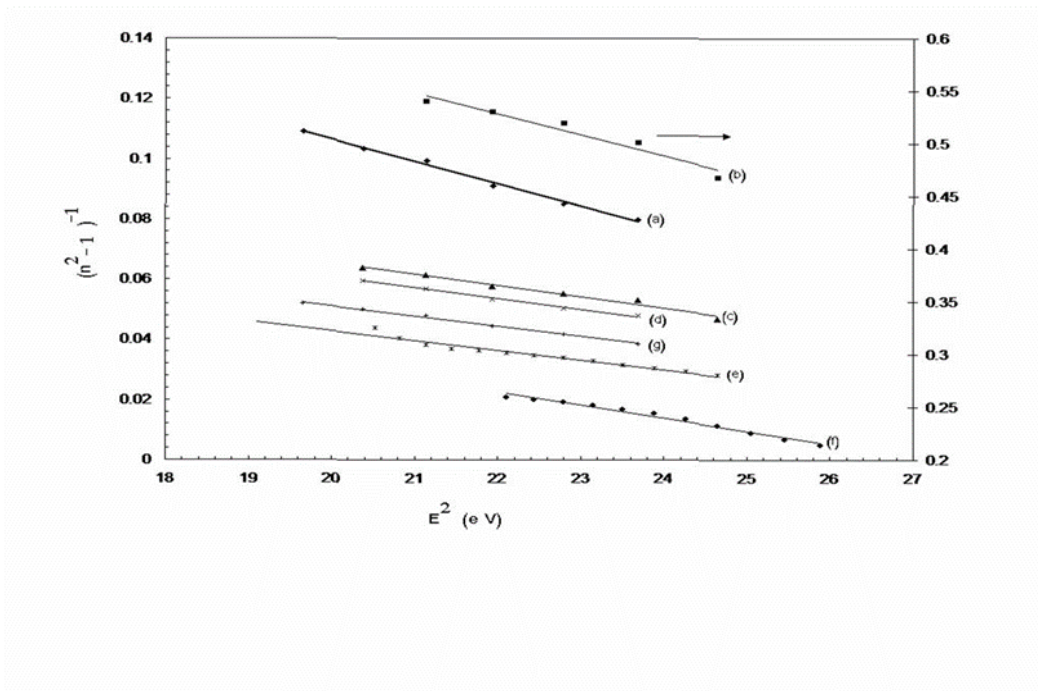


Figure 8 A plots of $(n^2-1)^{-1}$ as a function of photon energy ($h\nu$) for (a) pure gelatin (b) pure TGS (c) 2 (d) 4 (e) 6 (f) 8 and (g) 10 wt.% TGS.

On the other hand, the parameters of single-oscillator model E_0 and E_d are connected to M_{-1} and M_{-3} moments of the $\epsilon(E)$ optical spectrum, through the two relations[56]:

$$E_0^2 = \frac{M_{-1}}{M_{-3}} \tag{16}$$

$$E_d^2 = \frac{M_{-1}}{M_{-3}} \tag{17}$$

whererth moment of the optical spectrum is given by

$$M_r = \frac{2}{\pi} \int_{E_t}^{\infty} E_{\varepsilon_i}^r(E) dE \tag{18}$$

and E_t is the absorption threshold energy. The two moments M_{-1} and M_{-3} were calculated from the data on E_0 and E_d , and their values for pure gelatin and TGS and their composite samples are listed in Table 6.

Table 6 The two moments M_{-1} and M_{-3} of Gelatin, TGS and their composite sample

| Sample | M_{-1} (eV) ⁻² | M_{-3} (eV) ⁻² |
|-----------|--------------------------------|--------------------------------|
| Gelatin | 3.94 | 0.11 |
| TGS | 1.04 | 0.02 |
| 2wt.%TGS | 7.2 | 0.19 |
| 4wt.%TGS | 8.13 | 0.26 |
| 6wt.%TGS | 8.63 | 0.29 |
| 8wt.%TGS | 8.65 | 0.32 |
| 10wt.%TGS | 11.76 | 0.47 |

The single-oscillator model enables us to calculate the refractive index at infinite wavelength (n_{∞}), average oscillator wavelength (λ_0), and oscillator strength (S_0) through the relation[57].

$$\frac{n_{\infty}^2 - 1}{n^2 - 1} = 1 - \frac{\lambda_0^2}{\lambda^2} \tag{19}$$

Rearranging this equation yields

$$n^2 - 1 = \frac{S_0^2 \lambda_0^2}{(1 - \lambda_0^2) / \lambda^2} \tag{20}$$

where $S_0 = (n_{\infty}^2 - 1) / \lambda_0^2$. The values of n_{∞} and S_0 are derived from a linear plot of $(n^2 - 1)^{-1}$ versus $1/\lambda^2$ as seen in Fig. 9 and presented in Table 5.

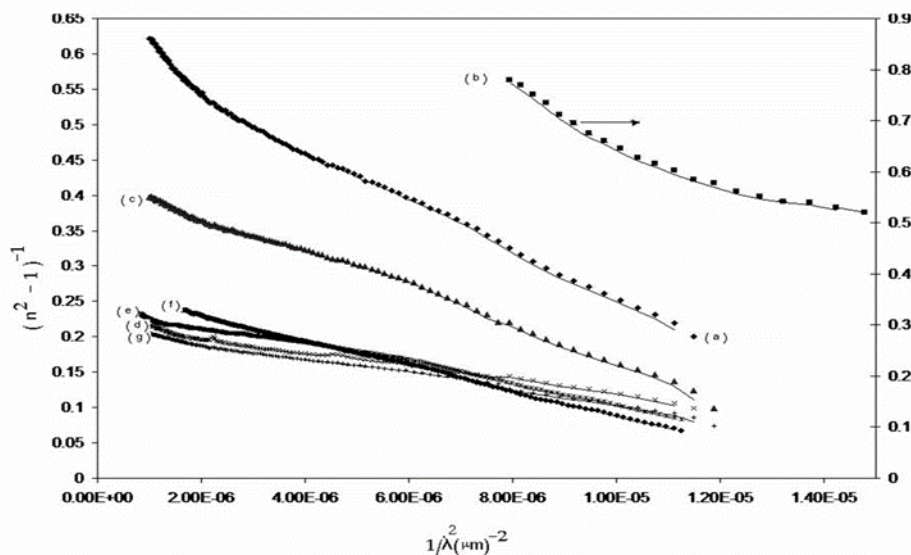


Figure 9 Relation between $(n^2-1)^{-1}$ and $1/\lambda^2$ for (a) pure gelatin (b) pure TGS (c) 2 (d) 4 (e) 6 (f) 8 and (g) 10 wt.%TGS.

4. CONCLUSIONS

From UV-visible studies, it is recognized that polymer/ferroelectric compositions ratio highly affect the electronic structure and molecular configuration of the composite matrix as seen from the pronounced changes in absorption spectra and confirmed by the calculated optical parameters. The allowed indirect transition is the most probable type of transition near the fundamental absorption edge of TGS/Gelatin composites. The sample 2wt.%TGS has the highest band tail and the lowest optical energy gap while the other composite samples are less band tails and highest optical energy gap. The compositional dependence of the refractive index can be caused by the interference phenomena due to domain structure, molecular orientation and processing conditions. The relatively high increase of the refractive index of the composition samples may be attributed to an increase in the valence density of charge carriers. The single oscillator parameters E_d , E_0 , n_∞ , λ_0 and S_0 have compositional dependence where

the dipole strength F and the strength of the intra band optical transition are enhanced by increasing the concentration of the ferroelectric material TGS into Gelatin.

References

- [1] V. E. Khutorsky and Sidney B. Lang *J. Appl. Phys.* 82 (1997) 25
- [2] J. R. Magariños and D. J. Coleman *Opt. Eng.* 24 (1985) 769
- [3] B. J. Chang, *Opt. Eng.* 19(1980) 642
- [4] R. T. Chen, W. Phillips, T. Jansson, and D. Pelka, *Opt. Lett.* 14 (1989) 892
- [5] R. T. Chen, M. R. Wang, and T. Jansson, *Appl. Phys. Lett.* 57 (1990) 2071
- [6] R. T. Chen, M. R. Wang, G. J. Sonek, and T. Jansson, *Opt. Eng.* 30 (1991) 622
- [7] Z. Z. Ho, R. T. Chen, and R. Shih, *Appl. Phys. Lett.* 61 (1992) 4
- [8] D. Damjanovic, A. S. Bhalla, and L. E. Cross, *Ferroelectr. Lett. Sect.* 11 (1990) 117
- [9] D. Damjanovic, A. S. Bhalla, and L. E. Cross, *Ferroelectrics* 109 (1990) 333
- [10] D. Damjanovic, A. S. Bhalla, and L. E. Cross, *IEEE Trans. Ultrason. Ferroelectr. Freq. Control* 38 (1991) 630
- [11] P.J.A. Sobral, F.C. Menegalli, M.D. Hubinger, M.A. Roques, *J. Food Hydrocolloids* 15 (2001) 423
- [12] R.A. Carvalho, C.R.F. Grosso, *J. Food Hydrocolloids* 18 (2004) 717
- [13] M. Thomazine, R.A. Carvalho, P.J.A. Sobral, *J. Food Science* 70 (2005) 172
- [14] F.M. Vanin, P.J.A. Sobral, F.C. Menegalli, R.A. Carvalho, A.M.Q.B. Habitate, *J. Food Hydrocolloids* 19 (2005) 899
- [15] P.V.A. Bergo, R.A. Carvalho, P.J.A. Sobral, F.R.S. Bevilacqua, J.K.C. Pinto, J.P. Souza, *J. Measurement Science and Technology* 17 (2006) 3261
- [16] I. Arvanitoyannis, E. Psomiadou, A. Nakayama, S. Aiba, N. Yamamoto, *J. Food Chemistry* 60(1997)593
- [17] Y. Pranoto, C.M. Lee, H.J. Park, *Lebensmittel-Wissenschaft und Technologie*, 40 (2007) 766
- [18] L.T. Lim, Y. Mine, A. Tung, *J. Food Science* 64 (1999) 616
- [19] N. Gontard, S. Guilbert, J.-L. Cuq, *J. Agricultural and Food Chemistry* 58 (1993) 206
- [20] Rose PJ, Mark HF, Bikales NM, Overberger CG, Menges G, Kroschwitz JJ, editors. *Encyclopedia of polymer science and engineering*, vol. 7, 2nd ed. New York, USA: Wiley, 1989:488-513.
- [21] R.B. Lal and A.K. Batra, *Ferroelect.* 142 (1993) 51
- [22] N. Nakatani, *Jpn. J. Appl. Phys.* 29 (1990) 2774
- [23] N. Nakatani, *Jpn. J. Appl. Phys.* 32 (1993) 4268
- [24] R.W. Whatmore, *Rep. Prog. Phys.* 49 (1986) 1335
- [25] A.K. Batra, Padmaja Guggilla, Dewanna Cunningham, M.D. Aggarwal, R.B. Lal, *Physica B* 371 (2006) 210
- [26] J. Novotny, J. Zelinka, F. Moravec, *J. Sensor Actuator A* 119 (2005) 300
- [27] Jiann-Min Chang, A.K. Batra, R.B. Lal, *J. Cryst. Growth Des.* 2 (2002) 431
- [28] S. Hoshino, Y. Okaya, and R. Pepinsky, *J. Phys. Rev.* 115 (1959) 323
- [29] R. LeBihan and G. Grandet, *J. Ferroelect.* 39 (1981) 117
- [30] D. Sun, X. Yu, Q. Gu, *J. Cryst. Res. Technol.* 34 (1999) 1255

- [31] Landolt-Bornstein, Crystal and Solid State Physics, New series, Group III, vol. 16b, Springer, New York, 1969, p. 223.
- [32] H.V. Alexandru, C. Berbecaru, F. Stanculescu, L. Pintilie, I. Matei, M. Lisca, *J.Sensor.Actuators A* 113 (2004)387
- [33] J.Novotny, L.Prokopova, and Z.Micka, *J.Cryst.Growth* 226 (2001)333
- [34] K.Meera, R.Muralidharan, P.Santhanaraghavan, R.Gopalakrishnan, and P.Ramasamy, *J.Cryst. Growth* 226 (2001)303
- [35] A.ArockiaLinson, AnbarasuPaulthurai, BalamuruganDamaraj, *Int.J.Nanoelectronics and Materials* 7(2014)93
- [36] W.Sakamoto, S.Kagesawa, D.K.andaD.Das-Gupta, *J. Mater .Sci.*33(1998)3325

- [37] C. Abrusci, A. Mart'ın-González, A. Del Amo, F. Catalina, , P. Bosch, T. Corrales J. *Photochemistry and Photobiology A: Chemistry*163 (2004)537
- [38] Diogo F. Vieira, C'esar O. Avellaneda, AgnieszkaPawlicka, *J. ElectrochimicaActa* 53(2007) 1404
- [39] K. Meera, A. Claude, R. Muralidharan, C.K. Choi, P. Ramasamy *J. Crystal Growth*285 (2005) 358
- [40] T. Balu, T.R. Rajasekaran, P. Murugakoothan, *J.Current Applied Physics*, 9 (2009)435
- [41] M.A. Omar, *Elementary solid state physics principles and applications*, Addison Wesley Publishing Inc., (1975).
- [42] J. Rodriguez, M. G'omez, J. Ederth, G.A. Niklasson, C.G. Granqvist, *Thin Solid Films*, 365 (2000)119
- [43] A.Abass and F.Al-Eithzn, *J.Phys.Chem.Solids*47(1986) 933
- [44] A.AbuEl.Fadl, *J.Cryst.Res.Technol.* 34(1999) 1047
- [45] A.AbuEl.Fadl, *J. Phys. and Chem. Solids*60 (1999)1881
- [46] A.Miller, "Handbook of optics", vol.1, McGraw Hill, New York, Chap. 9,(1994)
- [47] F.Urbach, *Phys.Rev.*92 (1953)1324
- [48] J. Tauc, in: F. Abeles (Ed.), *Optical Properties of Solids*, North Holland, (1969)
- [49] J.D.Dow and D.Redfield, *Phys.Rev.*B8 (1970) 3358
- [50] X.Tang, F.Hossain, K.Wongchotigul and M.G.Spence, *J. Appl.Phys.Lett.* 72(1998) 1501
- [51] N.F.Mott and E.A.Davis, " *Electronic processes in non-crystalline materials*", 2nded., Oxford university press, Oxford
- [52] J.Tauc, " *Optical properties of solids*", ed.S.Nuddelman and S.Mitra, New York: Plenum,(1969)
- [53] J. Tauc, in: F. Abeles (Ed.), *Optical Properties of Solids*, North Holland, (1969)
- [54] M. A Mahdi and S. K. J. Al-Ani, *Int. J. Nanoelectronics and Materlials*5 (2012) 11
- [55] E.M.Vogel, M.J.Weber, D.M.Krol, *J.Phys.Chem. Glasses* 32(1991) 25
- [56] S.H. Wemple, M. Di Domenico, *Phys. Rev. B*3 (1971)1338
- [57] F.Yakuphanoglu, M.Durmus, M.Okutan, O.Koysal, and V.Ahsen, *J. Phys. B* 373(2006) 262

© 2017 The Authors. Published by IFIA (<https://etn.iraqi-forum2014.com/>). This article is an open access article distributed under the terms and conditions of the Creative Commons Attribution license (<http://creativecommons.org/licenses/by/4.0/>).